
DAHITRA: DAMAGE ASSESSMENT USING A NOVEL HIERARCHICAL TRANSFORMER ARCHITECTURE

Navjot Kaur^a, Cheng-Chun Lee^b, Ali Mostafavi^{b,*}, Ali Mahdavi-Amiri^a,

^a School of Computing Science, Simon Fraser University,
British Columbia, Canada

^b Urban Resilience.AI Lab, Zachry Department of Civil and Environmental Engineering,
Texas A&M University, College Station, TX

* correponding author, email: amostafavi@civil.tamu.edu

ABSTRACT

This paper presents DAHiTra, a novel deep-learning model with hierarchical transformers to classify building damages based on satellite images in the aftermath of hurricanes. An automated building damage assessment provides critical information for decision making and resource allocation for rapid emergency response. Satellite imagery provides real-time, high-coverage information and offers opportunities to inform large-scale post-disaster building damage assessment. In addition, deep-learning methods have shown to be promising in classifying building damage. In this work, a novel transformer-based network is proposed for assessing building damage. This network leverages hierarchical spatial features of multiple resolutions and captures temporal difference in the feature domain after applying a transformer encoder on the spatial features. The proposed network achieves state-of-the-art-performance when tested on a large-scale disaster damage dataset (xBD) for building localization and damage classification, as well as on LEVIR-CD dataset for change detection tasks. In addition, we introduce a new high-resolution satellite imagery dataset, Ida-BD (related to the 2021 Hurricane Ida in Louisiana in 2021, for domain adaptation to further evaluate the capability of the model to be applied to newly damaged areas with scarce data. The domain adaptation results indicate that the proposed model can be adapted to a new event with only limited fine-tuning. Hence, the proposed model advances the current state of the art through better performance and domain adaptation. Also, Ida-BD provides a higher-resolution annotated dataset for future studies in this field.

Keywords Damage classification, Change detection, Domain adaptation, Satellite imagery, UNet, Attention, Transformers

1 INTRODUCTION

Rapid and automated damage assessment of buildings and infrastructure in the aftermath of disasters is critical to expedite emergency response and resources. Damage assessments done by ground crews can be time-consuming and labor-intensive (Spencer et al., 2019). To investigate expediting building damage assessments, studies have applied computer-vision techniques on building images (N. Wang et al., 2020; Zou et al., 2022), high-resolution aerial imagery (Cheng et al., 2021; Fujita et al., 2017), and satellite imagery (Cao & Choe, 2020; McCarthy et al., 2020; Tong et al., 2012). While aerial imagery can capture more details of the condition of buildings due to lower flying altitudes than satellite imagery, it requires extensive local planning and provides a smaller area of building coverage than satellite imagery. Satellite imagery, which provides near real-time and high-coverage information, offers opportunities to assist in large-scale post-disaster building damage assessments (Corbane et al., 2011). Studies (Hao et al., 2021; Shen et al., 2022; C. Wu et al., 2021) have shown that by leveraging satellite imagery and deep learning, the process of damage assessments can be accelerated with the generation of high-quality building footprints and damage-level classification

for each building. The majority of existing models are built using a single dataset (xBD) (Gupta et al., 2019) but have not been tested on datasets that include newly damaged areas. In this work, we overcome these limitations by creating a novel deep-learning technique to perform damage classification, building segmentation tasks, and testing of the model on a new and higher-resolution dataset related to building damage, Ida-BD, in Louisiana in the aftermath of Hurricane Ida.

The most common approach for building damage assessment using satellite imagery is to pose the problem as a combination of segmentation and classification tasks and to train deep-learning models on pre-disaster and post-disaster satellite images. Many researchers have utilized convolutional neural networks (CNNs) to achieve models with acceptable performance (Gupta & Shah, 2021; Hao et al., 2021; C. Wu et al., 2021). For example, Weber and Kané (2020) considered building damage assessment as a semantic segmentation task in which damage levels are assigned to different class labels. Pre- and post-disaster image channels are concatenated into a single input, relying on the model to differentiate between the channels of pre- and post-disaster conditions, which complicates the learning process.

The problem of damage classification can be also modeled as change detection where the change is detected over a period of time with a pair of pre- and post-disaster images. Standard practice in the existing literature is to use a CNN-based network with a two-branch architecture for pre- and post-disaster images and directly concatenating the learned features to process pixel localization and classification Gupta and Shah (2021); Hao et al. (2021); C. Wu et al. (2021).

We argue that directly concatenating features complicates the task of localizing pixels for damage assessment; the network should concentrate on the changes between pre- and post-disaster images. Therefore, our classifier works on the *difference* between features. Since pre- and post-disaster images are usually obtained at different times and under different lighting or weather conditions, to find meaningful and unbiased difference, both images should be mapped to a *common domain*. Therefore, we used *transformer blocks* that map the features of post- and pre-disaster images into a common domain to better assess the difference. In addition, as damage is typically at different scales, features should be obtained at multi-resolutions. As a result, in our network, we take advantage of UNet-based structures to learn features at different scales and we build a *hierarchy* of those features obtained at different scales to localize and classify the changes between two images. In Section 5, we performed ablation studies to validate our design choices, and we also compared our method with the state-of-the-art techniques and demonstrated that our method outperforms the alternatives.

Every disaster is unique although they may share some similar characteristics. For example, the building damage caused by a hurricane may not be the same as the damage caused by another hurricane in the future. Therefore, using models based on images directly from previous disaster events to assess the damage of a new event requires the models to be tested on new datasets to evaluate the adaptation performance of the models. This has been a major limitation in previous studies since most of the existing models were created based on the xBD dataset with limited or no adaptation performance testing. To address this limitation, we introduced a new dataset, Ida-BD, with 87 image pairs (1024 x 1024) with a very high resolution (0.5 m/pixel) from Hurricane Ida (2021) in Louisiana. Hurricane Ida brought the strongest winds ever recorded in Louisiana and heavy rains, which caused an estimated \$18 billion in building damage and at least 30 fatalities in Louisiana (Beven II et al., 2022). Since the near-real-time damage assessment face the scarcity of labeled datasets, already available datasets can be used for training, and some domain adaptation techniques or fine-tuning can be applied to obtain satisfactory results on the newly damaged areas with scarce data. As a result, Ida-BD dataset can serve as a benchmark for domain adaptation from larger datasets like xBD. In this paper, we also provide a baseline for the domain adaptation task using a simple transfer learning method. Accordingly, the contributions of this work are as follows:

- We present a hierarchical UNet-based architecture which uses transformer-based difference to perform well on both the damage classification and building segmentation tasks.
- We introduce a new dataset, Ida-BD, for evaluating the model’s adaptation performance and provide a baseline for damage assessment task.
- We provide a simple approach for effective domain adaptation and demonstrate the usefulness of the new dataset and efficacy of the proposed network for transfer learning.

The rest of the paper is organized as follows. We first discuss related works in the field of building damage classification and change detection using satellite images in Section 2. In Section 3, we detail our model architecture along with loss functions and training settings. Section 4 provides an overview of the datasets used for evaluation and the results are presented in the Section 5. We offer conclusions in Section 6.

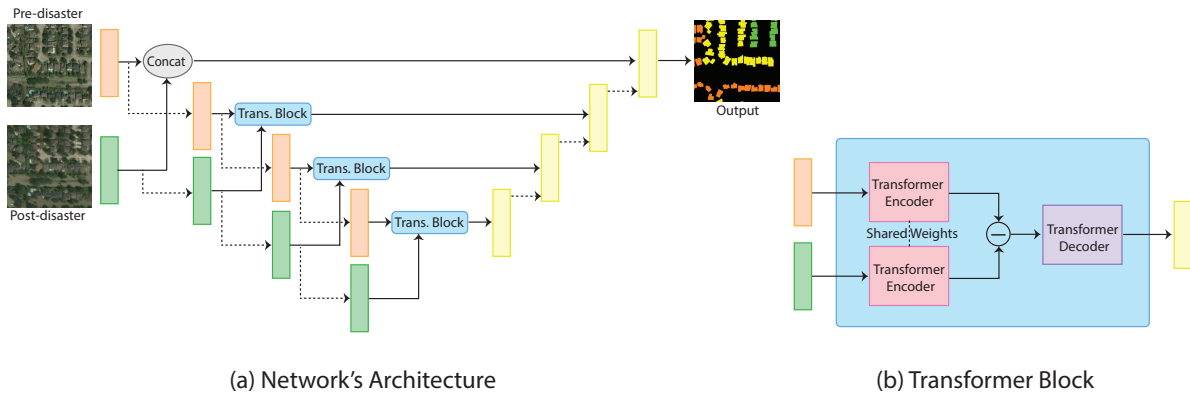


Figure 1: The model architecture for damage detection and classification. A pair of pre-disaster and post-disaster images is fed into an encoder made up of stacked convolution blocks (orange and green layers), where each block downsamples the features space (dashed lines). The output from each block of pre- and post-disaster image encoders is passed jointly (solid lines) into the transformer block, which maps the spatial features into feature domain and then take the difference followed by transformer decoder to map the features back into spatial domain. Next the output mask is hierarchically built by up-sampling (dashed lines) and concatenating the features from lower dimension to higher dimension layers.

2 Related work

This section discusses recent methods used for building damage classification using satellite images. Since the xView2 challenge (Gupta et al., 2019) in 2019, many researchers have tried various techniques from Siamese networks (Hao et al., 2021; C. Wu et al., 2021), to convolutional networks (Gupta & Shah, 2021; Weber & Kané, 2020), to attention mechanisms (Shen et al., 2022) to solve the problem of damage classification.

Earlier models, such as Hao et al. (2021), combined the UNet model with the Siamese architecture where the UNet model learns the semantic segmentation of buildings and the Siamese network focuses on the damage classification by comparing the segmented outputs. C. Wu et al. (2021) further developed the model by using attention-based UNet where attention is applied to the incoming layers from the encoder module before fusing with the up-sampled features in the decoder. These architectures rely on global features learned from pre- and post-disaster images that are then merged to learn the change (here, damage) at the final stage. Since the majority of parameters prioritize learning the global features for a single image, this setting makes it difficult for the model to benefit from the multi-task supervision required to learn the change.

Gupta and Shah (2021) drew insights from DeepLabv3+ and adapted it for damage classification by using a backbone of Dilated ResNet and Atrous Spatial Pyramid Pooling module to generate multi-scale features from pre- and post-disaster images, then comparing their differences to learn the temporal change. Similar to Siamese networks, a large set of layers of this model focus on learning the changes in images separately, which limits the learning capacity of the last few layers to make an efficient change detection. Additionally, this model uses multi-scale features to capture input image variations, but these features are later simply concatenated and passed into a convolutional block for the final output. Because the change itself could be of varying resolutions, a hierarchical or multi-scale analysis would be useful to generate a better quality temporal change mask.

More recently, researchers modeled the temporal relation between pre- and post-disaster images using attention mechanisms. For instance, Shen et al. (2022) used cross-directional attention in a two-stage framework for building segmentation and damage assessment. After modeling for building segmentation using single UNet branch, the pre- and post-disaster images are fed into two separate branches and cross-directional attention is used to exchange information between the two parameter branches. We note that we can explicitly enforce the model to learn the temporal difference by mapping the pre- and post-disaster features from the spatial domain to another feature domain then taking their absolute difference. The self-attention can be used to map the features from spatial to the feature domain, which can be efficiently applied through transformers. The transformers, although not specifically used for building damage classification tasks, have been successfully applied for building change detection on satellite images. It can be seen that the damage classification problem (multi-class classification) is similar to change detection (binary classification) by viewing the level of damage as change, although the damage classification problem is more difficult due to the higher target dimensionality. Moreover, the damage classes are not mutually exclusive and distinct as compared to change

detection where the presence of new infrastructure directly indicates change. For instance, there is no definitive way to classify the roof damage as major damage instead of minor damage.

Among the state-of-the-art methods for change detection, Chen et al. (2022) introduced bi-temporal image transformer (BiT) to model pre- and post-change contexts into visual semantic tokens using spatial attention. The transformer encoder is then used to learn the temporal context between the two token sets, followed by a transformer decoder projecting the features back to the pixel-space. An explicit difference is then taken on the features to generate the change mask. Although this model has significantly outperformed previous models for change detection, its performance is limited by the feature space of the visual semantic tokens. The tokens are low-dimension features generated by a CNN module, and the transformer encoder and decoder have just this information to learn change and reconstruct a high-dimensional output. Also, the final change prediction mask is generated by a single-step up-sampling from the very low-resolution feature space (1/4th of the final resolution) which makes it difficult to generate high-resolution change masks.

Another recent work for change detection by Bandara and Patel (2022), which is the closest approach to our method, uses hierarchically structured transformer encoder modules along with multi-layer perceptron (MLP) decoders in a Siamese network architecture. In this network, transformers function as feature extractors and are applied on all scales of features; however, as analyzed in B. Wu et al. (2021), the transformers are inefficient at the early stages, and the convolutions are better at extracting low-level features. Therefore, we instead use the convolutions as the base feature extractors and then apply the transformers to map these features from different temporal domains to a common domain. Also, in the work by Bandara and Patel (2022), the difference module is based on concatenation of pre- and post-change features from the transformer encoder output followed by a single-step accumulation of change features from different resolutions. However, the hierarchical reconstruction of the output map provides the model more guidance for global context and hence produces better high-resolution results.

3 Method

We propose a novel neural network called DAHiTrA for multi-class change detection for the purpose of building damage assessment. DAHiTrA is based on UNet and transformers to learn hierarchical features of pre- and post-disaster images. Transformers offer common domains at multiple scales for pre- and post-disaster images (Figure 1). Here we explain DAHiTrA’s architecture and the utilized loss functions. We also discuss how to use DAHiTrA for domain adaptation on unseen small satellite image datasets.

3.1 Model architecture

Our model is motivated by the strengths of visual transformer and UNet architecture, which are established for effectively learning context and image segmentation tasks, respectively. We first trained UNet for building the segmentation task on the xBD dataset using pre-disaster images and intermittently giving the post-disaster images. This information is later used as a backbone to provide the initial encoding features. We further encode these features using transformers and take the difference in the feature domain and then pass it to the transformer decoders to map the features back in the spatial domain. In the decoding stage, we hierarchically build the output mask by up-sampling and concatenating the features from lower to higher dimension layers followed by convolutional layers to avoid any artifacts due to up-sampling. This leads to hierarchical development of the damage output mask, which performs well on both the classification and segmentation tasks.

3.1.1 Loss function

We used a class-weighted loss function provided in Equation 1 with a combination of focal loss and dice loss to perform well for the classification task on the unbalanced dataset. A total of five classes were considered: background (0), no damage (1), minor damage (2), major damage (3) and destroyed (4), and weights w_i were assigned as per the pixel distribution of the classes in xBD dataset (Table 1). The focal loss $\mathcal{L}_{foc(i)}$ is used to further address the class imbalance where a modulating term is applied to the cross-entropy loss function to focus the learning on hard mis-classified examples. The second loss is dice loss $\mathcal{L}_{dice(i)}$, which tries to maximize the overlap between predicted and ground-truth boundaries. The denominator considers the total number of boundary pixels at global scale, while the numerator considers the intersection, implicitly capturing local behaviour.

$$\begin{aligned}
\mathcal{L}_{tot} &= \sum_i w_i (\mathcal{L}_{foc(i)} + \alpha \mathcal{L}_{dice(i)}) & i \in \{0, \dots, 4\} \\
\mathcal{L}_{foc(i)} &= \sum_i -(1 - p_i)^\gamma \log(p_i) & i \in \{0, 1\} \\
\mathcal{L}_{dice(i)} &= 1 - \frac{2 |\tilde{c} \cup c|}{|\tilde{c} \cap c|} & c \in \{0, 1\}
\end{aligned} \tag{1}$$

Table 1: Class-wise pixels count distribution in xBD dataset and the corresponding weights used in training. The notation used: 0-Background, 1-No damage, 2-Minor damage, 3-Major damage, 4-Destroyed

	0	1	2	3	4
Pixels count	96	2.7	0.1	0.1	0.1
Weight assigned	0.01	0.1	0.7	0.7	0.7

Table 2: Class-wise pixel count distribution in xBD dataset and Ida-BD dataset. The notation used: 0-Background, 1-No damage, 2-Minor damage, 3-Major damage, 4-Destroyed

	0	1	2	3	4
xBD	96.1	2.7	0.1	0.1	0.1
Ida-BD	81.7	11.9	4.6	1.6	0.05

3.1.2 Training settings

The model is trained using Adam optimizer with learning rate starting with value of 1e-4, which is gradually reduced by factor of 0.6 following a multi-step learning rate scheduler. For the xBD dataset, the model takes in 1024 x 1024 images as input and is trained using a batch size of 8 for 50 epochs. For the LEVIR dataset, the model takes in 256 x 256 cropped images and is trained using a batch size of 16 for 200 epochs. Geometric and photometric data augmentations are heavily used to make the model robust to variations and noise in the dataset. We hold 10% of the data for validation and train on the remaining set.

3.1.3 Domain adaptation

To use the model on small datasets like Ida-BD (introduced in Section 4.2), we use a simple transfer learning approach to fine-tune our model on the new dataset. The diverse nature of satellite imagery captured from different locations, terrains, and weather conditions makes machine-learning algorithms difficult to generalize, which means the model trained on the xBD dataset does not generalize well for other datasets. Additionally, training a model on small datasets from scratch is difficult for the highly complex tasks such as damage classification. Domain adaptation algorithms have been proposed (M. Wang & Deng, 2018) to enable models trained on images from one dataset (source) to work on images from another dataset (target). Here, we use the discrepancy-based method to fine-tune the network with labeled target data to diminish the domain shift. We ran the pre-trained model from xBD dataset on the target dataset for 10 epochs using a fixed learning rate of 1e-6.

4 Datasets

The xBD dataset Gupta et al. (2019) was used for model training and testing for disaster damage detection and classification tasks. Later, we introduced a new dataset of higher resolution (but smaller size) from Hurricane Ida for damage assessment and explore the domain adaptation from xBD to this data. Additionally, we also use LEVIR-CD dataset to evaluate the model for the change detection task.

4.1 xBD

We use the xBD dataset (Gupta et al., 2019) in this study for disaster damage detection and classification tasks. The xBD dataset is a large-scale building damage dataset that publicly available by providing high-resolution (0.8 m/pixel) satellite imagery with building segmentation and damage level labels. The xBD dataset provides geo-registered pairs of pre- and post-disaster images collected from 19 disaster events such as hurricanes and floods with an image size of 1024 x 1024 pixels. The dataset uses polygons to represent building segments and provides four damage categories—no damage, minor damage, major damage and destroyed—for each building. We make use of the tier 1 and tier 3 data

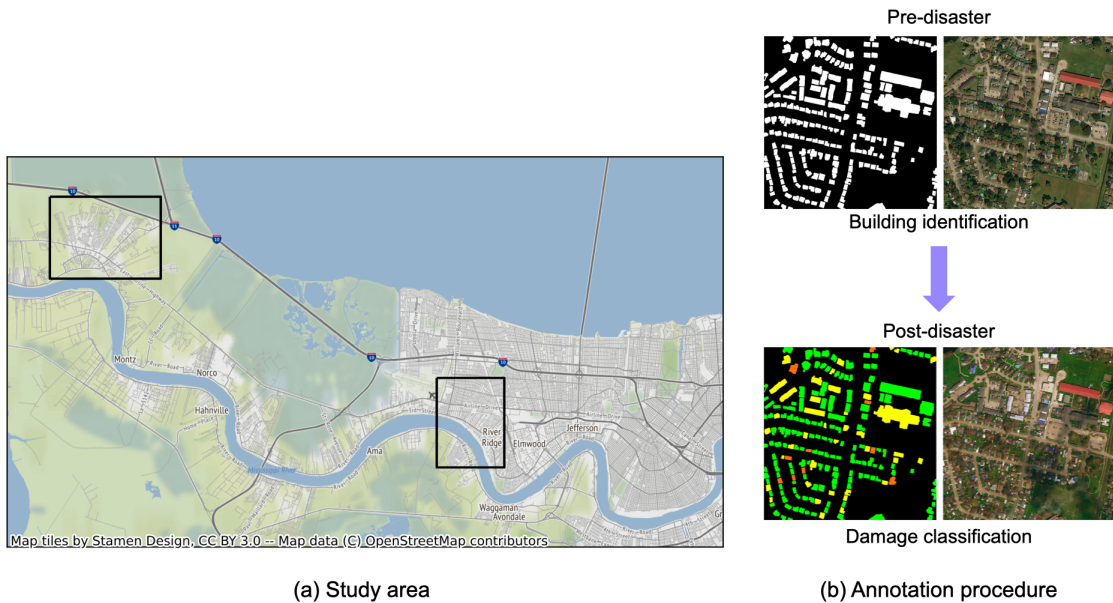


Figure 2: (a) Location of Ida-BD near New Orleans, Louisiana, and (b) example of the annotation of buildings and damage levels

partitions where the labels are available. Using stratified sampling based on the damage class distribution, 10% of this data is kept aside for validation, and another 10% for the final testing purpose. The rest of the data is used for training the model.

4.2 Ida-BD

We offered a new dataset, Ida-BD, obtained from the WorldView-2 (WV2) satellite with very-high-resolution images taken in November 2020 and July 2021 for pre-disaster and September 2021 for post-disaster. The satellite imagery was collected close to New Orleans, Louisiana, one of the most heavily impacted areas during Hurricane Ida in late August 2021 (Figure 2a). The WV2 satellite provides panchromatic images with spectral resolution of 450–800 nm and spatial resolution of 46 cm. The panchromatic images in this dataset were first orthorectified by Apollo Mapping to 0.5 m/pixel. We then created 87 image pairs (pairs of pre- and post-disaster images at the same location) with a size of 1024 x 1024 pixels. The resolution of these images was finer than the ones in the xBD dataset. Similar to xBD, we used polygons to represent building segments and provided four damage categories. All annotations were done by the in-house team with quality control procedures using Labelbox (Labelbox, 2022). The annotation procedure is shown in Figure 2b. We first annotated building polygons in pre-disaster images to avoid incorrect building boundaries due to damage. Then, by overlapping the annotation of building boundaries, we classified building damage for each building based on post-disaster images. All annotations, including building boundaries and damage levels, were reviewed several times by experts on the team. The comparison of damage class distribution in xBD and Ida-BD datasets is shown in Table 2. Ida-BD shows more damaged buildings at all levels in terms of pixel counts compared with xBD except for the class of destroyed buildings. Due to the small size of the dataset, it is hard to use it directly for training a model from scratch; therefore, we leveraged domain adaptation using a pre-trained model on the xBD dataset for training and evaluation on this dataset. Since the xBD dataset includes various disaster types, the class distribution of xBD dataset is quite different from Ida-BD dataset. To address this shift in target distribution, we updated the class weights in the loss function according to the new distribution. We also use aggressive data augmentation for scaling and normalization to model transfer knowledge from the dataset with different resolution and RGB distribution. We have made this dataset publicly available at DesignSafe-CI (Lee et al., 2022).

4.3 LEVIR-CD

LEVIR-CD consists of bi-temporal satellite images from Texas capturing significant land-use changes such as new construction or building decline. This dataset has 637 pairs of very-high-resolution (VHR, 0.5 m/pixel) satellite imagery with periods of 5 to 14 years and a size of 1024 x 1024 pixels. There are nearly 31K building instances within this dataset, including various building types such as warehouses, garages, and apartment complexes. This dataset provides

binary masks as labels with values 1 for changed and 0 for unchanged. Similar to the split for the xBD dataset, we keep aside 10% of the data for validation and another 10% for testing while using the rest for model training.

5 Evaluation

In this section we present the evaluation results of the model on the datasets listed in Section 4. We first share the metrics used for the evaluation and then present the qualitative and quantitative results. Later we discuss ablation studies to examine the impact of components of our model and loss functions.

5.1 Metrics

We used the XView2 Challenge metrics to evaluate our results for the xBD dataset. The metrics include a weighted average of the F1-scores of building segmentation results and a harmonic mean of the F1-scores of class-wise damage classification results:

$$Score = 0.3 * F1_{Loc} + 0.7 * F1_{Class} \quad (2)$$

$$F1_{Loc} = \frac{2 | X \cup Y |}{| X | \cap | Y |}$$

$$F1_{Class} = \frac{1}{\frac{1}{F1_i} + \dots + \frac{1}{F1_n}}$$

Here, $F1_{Loc}$ is the F1-Score for building segmentation. X and Y denote background and buildings interchangeably. $F1_i$ denotes class-specific F1 scores for each damage level. Since this metric heavily penalizes overfitting on the over-represented classes and given that xBD dataset is heavily skewed towards no-damage class, it is a challenging metric to use for evaluation.

5.2 Quantitative and qualitative results

Here we discuss the results for three tasks: damage detection and classification, change detection, and domain adaptation tasks. We evaluate the results for these tasks on xBD dataset, LEVIR dataset, and Ida-BD dataset.

5.2.1 Results for damage classification

We tested our model on the xBD dataset for the damage detection and classification tasks by comparing the F1-score and IOU metrics. We compared the results with Siamese UNet (C. Wu et al., 2021), which serves as a baseline for most of the works in damage detection. We compared with Dual-HRNet (Ku et al., 2020), which was one of the top-performing architectures in xview2-challenge (Gupta et al., 2019). Additionally, we compared with the numbers published by the attention-based models RescueNet (Gupta & Shah, 2021) and BDANet (Shen et al., 2022). We observed that our model performs well on all the metrics, (Table 3). Considering class-wise performance individually, BDANet performs better for major and destroyed classes. We note, however, that our model performs well in all classes jointly and gives higher overall F1-score and IOU. The qualitative results are displayed in Figure 3, where our model assigns the same damage level to almost all pixels within a building boundary, in contrast to Siamese UNet and Dual-HRNet.

5.2.2 Results for change detection

We evaluated the performance of change detection on LEVIR dataset and compared it against the recent transformer-based networks proposed by Chen et al. (2022) and Bandara and Patel (2022). Our model performs significantly better in both overall F1-score and IOU metrics, as demonstrated in Table 4. In addition, we observed that adding a convolution layer after every merge of outputs from the transformer decoder and lower layer provides smoother results and fewer artifacts. The accuracy achieved under this setting is slightly lower than our final model, though higher than other recent works. The qualitative results are displayed in Figure 4, where we can see that the model produces finer building boundaries and captures a few additional buildings that had been missed by other models.

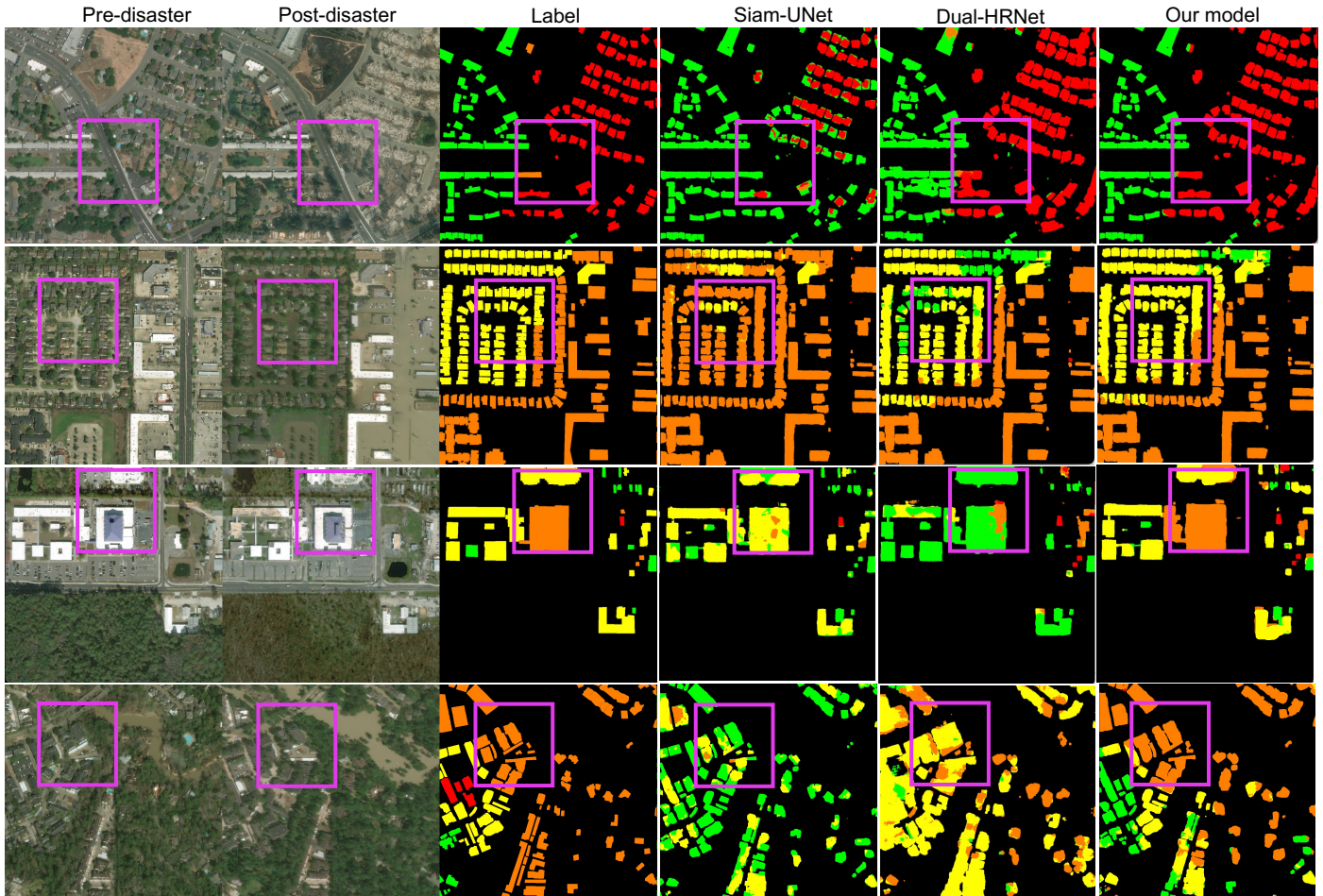


Figure 3: Qualitative results for damage classification (evaluation on xBD dataset). As highlighted in the boundary boxes, our model assigns more accurate damage level to almost all pixels within a building boundary as compared to Siamese UNet and Dual-HRNet

Table 3: Average quantitative results for damage classification on xBD dataset. Our model outperforms the state-of-the-art methods in the overall IOU and F1-score metrics as well as class-specific F1-scores for minor damage class and no-damage class. Although BDANet performs better for major damage and destroyed classes, our model has higher overall scores.

Model	Score	IOU	F1-Score	Class F1-scores			
				No Damage	Minor Damage	Major Damage	Destroyed
Siam-UNet	0.743	0.824	0.709	0.955	0.576	0.744	0.662
Dual-HRNet	0.769	0.834	0.741	0.898	0.590	0.737	0.809
RescueNet	0.766	0.840	0.735	0.883	0.563	0.771	0.808
BDANet	0.806	0.864	0.782	0.925	0.616	0.788	0.876
Ours	0.819	0.872	0.796	0.978	0.711	0.765	0.772

5.2.3 Results for domain adaptation

To evaluate the model adaptation performance on the Ida-BD dataset, we experimented with three training settings for our model using Siamese UNet as a baseline model. First, we trained the model on Ida-BD data from scratch and tested it. In the second setting, we initialized the model with weights from the pre-trained model on xBD data and compared

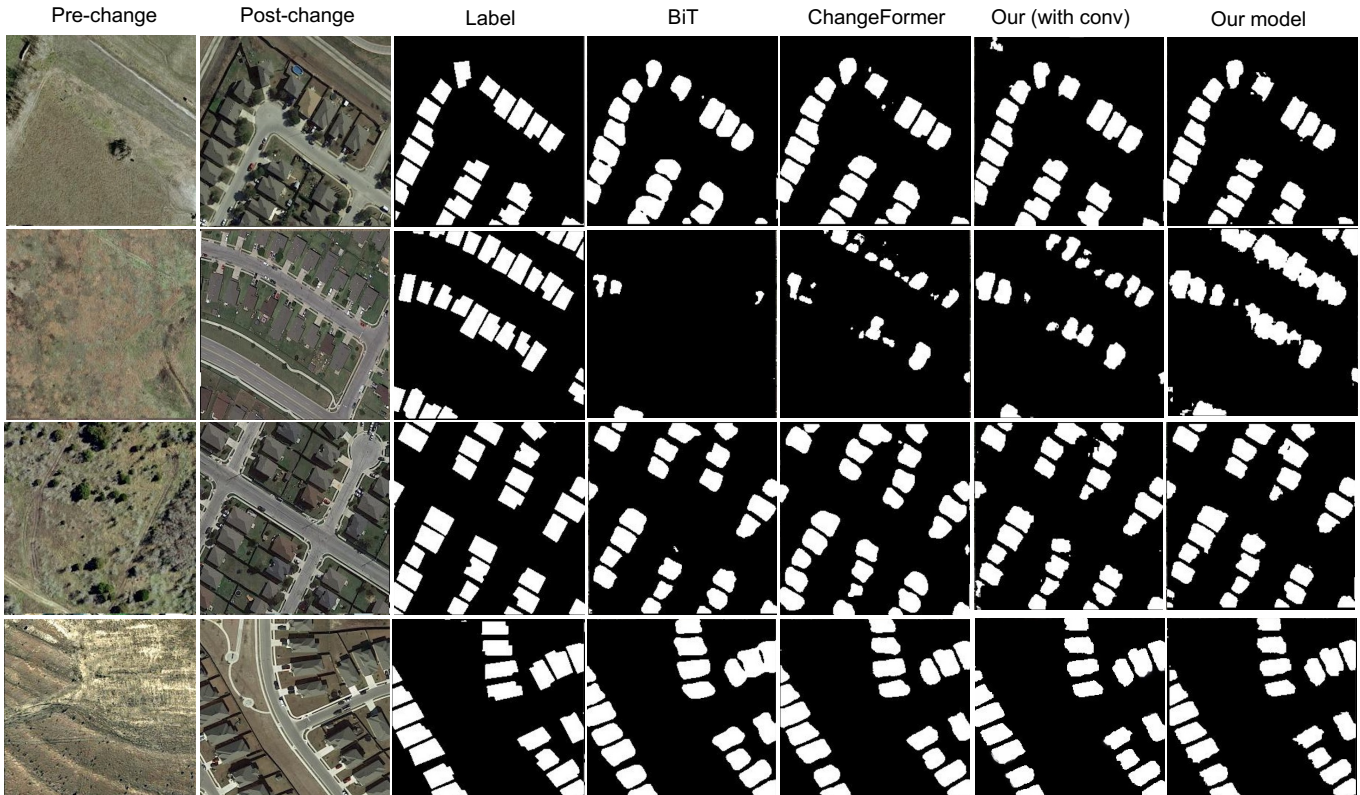


Figure 4: Qualitative results for change detection (evaluation on LEVIR-CD dataset)

Table 4: Average quantitative results for change detection on LEVIR-CD dataset. Our model performs significantly better than the state-of-the-art methods in overall F1-score and IOU as well class-specific F1-scores.

Model	IOU	F1-Score	Class F1-scores	
			0 class	1 class
Siam-UNet	0.813	0.859	0.987	0.788
BiT	0.829	0.899	0.990	0.807
Changeformer	0.828	0.898	0.990	0.806
Ours + with conv	0.833	0.901	0.991	0.812
Ours	0.842	0.908	0.991	0.825

its performance. Finally, we evaluated the pre-trained model directly without any fine-tuning on the Ida-BD dataset. Since the percentage of destroyed category is relatively lower than the rest of the classes (Table 2), we merged the destroyed class with major damage class and thus framed the problem as four-class classification (i.e., background, no damage, minor damage, major damage) for the fine-tuning. As shown in Table 5, the best performance was obtained by initializing the model with weights from the network trained on xBD data are then fine-tuned on the Ida-BD dataset. Pre-training on the large-scale xBD dataset provides the model a good prior, and the model is able to better generalize. The qualitative results are displayed in Figure 5.

5.3 Ablation studies

In this sub-section, we discuss few experiments on the impact of different loss functions and various components of our model.

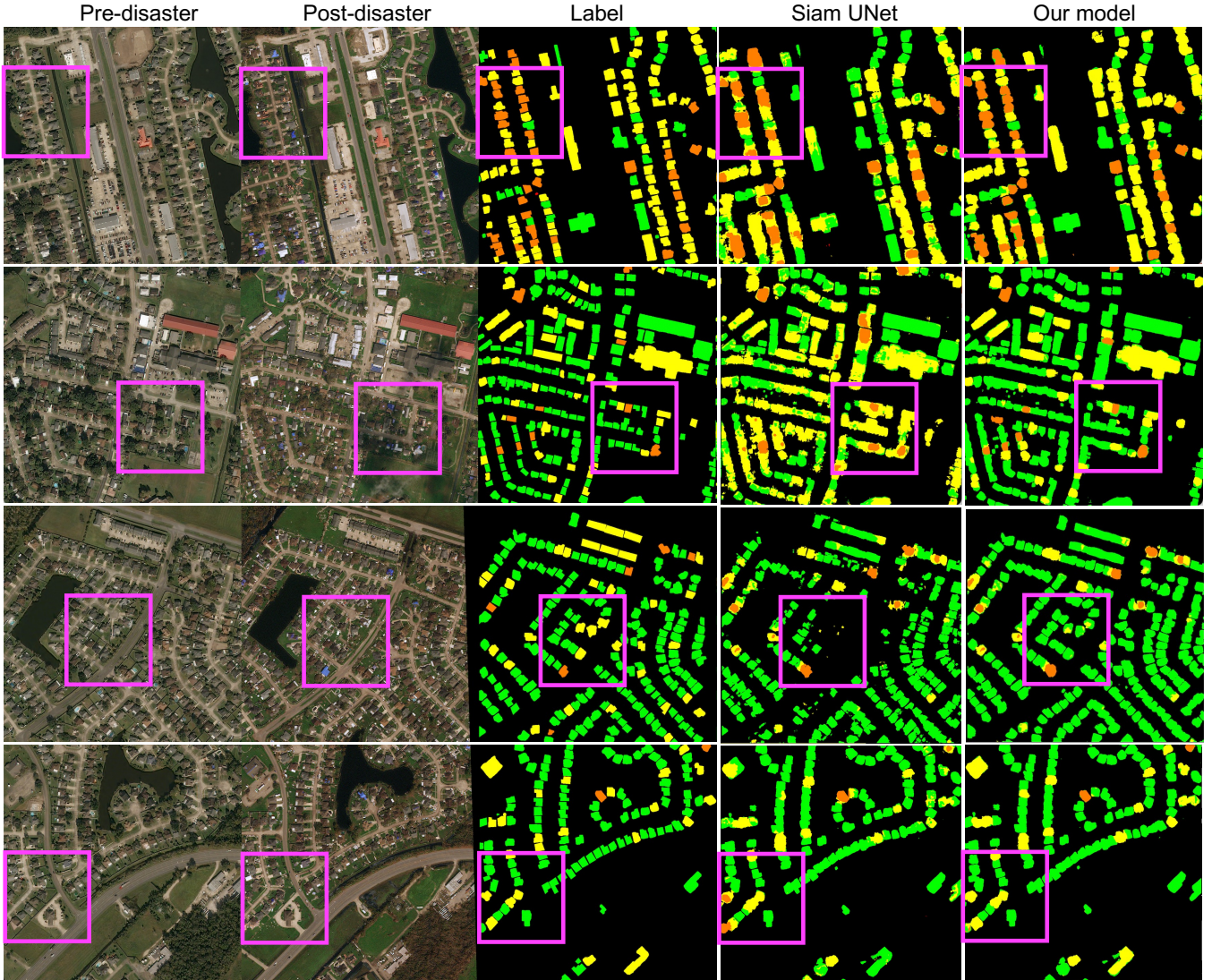


Figure 5: Qualitative results for domain adaptation (evaluation on Ida-BD dataset). Our model assigned significantly more accurate damage classes than Siamese UNet. Please compare the highlighted boxes as a reference.

Table 5: Domain adaptation on Ida-BD dataset. We experimented using three settings: (1) We trained the model on Ida-BD data (source and target) from scratch. (2) We initialized the model with weights from the pre-trained model on xBD data (source) and fine-tune on Ida-BD data (target). (3) We tested the model trained on xBD data (source) on Ida-BD (target) without target knowledge. The second setting performs the best for both the models while our model performs better than Siam-UNet in each of the settings in terms of F1-score and IOU.

Model	Pre-training	Training	IOU	F1-Score	Class F1-scores		
					No Damage	Minor Damage	Major Damage
Siam-UNet	-	Ida	0.697	0.472	0.906	0.313	0.483
	xBD	Ida	0.748	0.507	0.846	0.322	0.609
	xBD	-	0.584	0.307	0.916	0.208	0.251
Ours	-	Ida	0.778	0.541	0.916	0.384	0.538
	xBD	Ida	0.805	0.585	0.910	0.439	0.577
	xBD	-	0.674	0.023	0.881	0.617	0.008

Table 6: Impact of loss functions (xBD data).

Loss function	IOU	F1-Score
Focal + Dice	0.816	0.796
Focal + Dice + Ordinal	0.807	0.791
Buildings only Cross-entropy	0.798	0.803

Table 7: Effect of the number of transformer layers used (LEVIR data).

Number	IOU	F1-Score
0	0.818	0.843
1	0.837	0.897
2	0.843	0.903
3	0.842	0.908
4	0.838	0.901

5.3.1 Loss functions

We experimented with different combinations of loss functions (Table 6). The localization-aware loss (Gupta & Shah, 2021) gave better F1-scores for damage classes where pixels are accounted for in the cross-entropy loss calculation only in the presence of buildings. The segmentation results, however, were relatively poor, and we had to depend on segmentation masks generated from the pre-trained UNet model. We also tried ordinal loss in the form of mean square error between the ground truth and predicted output for buildings only by converting the values from a scale of 1 to 4 to the scale of 0 to 1. This loss did not work well for our task, which could be because of the highly imbalanced and sparse class distribution. The weighted sum of focal and dice loss provided the best performance in class-wise F1-scores as well as building boundary precision, since the former explicitly addresses the class imbalance and the latter ensures crisp building boundaries.

5.3.2 Transformer layers

We experimented with adding different numbers of transformer blocks between encoder and decoder; three iterations gave us the best results. We observed that adding transformer blocks at all levels, except the highest resolution layer, provided an incremental improvement in accuracy. An addition transformer block in final layer does not perform well, which could be because the input dimension is very high and it becomes hard for transformers to learn in this space, as discussed in B. Wu et al. (2021). Hence we used only the convolutional layer in the highest resolution layer. On the other hand, if the transformer is not used in any of the layers, the performance highly degrades, indicating the importance of transformer-encoded features. The test result values from the LEVIR-CD dataset are shared in the Table 7. Also, using a combination of transformer encoder and decoder along with the difference module, instead of just transformer encoder followed by difference module, provided a bump of accuracy by 0.8% for xBD dataset.

6 Concluding Remarks

With the growing number of disasters and limitations in trained human personnel to perform on-the-ground damage assessments, rapid and automated assessment of building damages is a critical step for disaster response. While a growing body of literature has shown the potential of using satellite imagery in deep learning models for automated damage assessment, our work was motivated by the need for models providing better performance than the existing ones and can be adapted in new disasters. To this end, we presented a coupled UNet architecture which uses transformer-based difference to perform well on both the damage classification and building segmentation tasks. We applied attention on the difference of the transformer encodings in the feature domain instead of the traditional spatial domain. We hierarchically built the output damage mask by up-sampling and concatenating the low dimension features with higher dimension features. The proposed method yield state-of-the-art results on xBD dataset and LEVIR-CD dataset for damage classification and change detection tasks respectively. We also provided a new baseline for the domain adaptation task on the Ida-BD dataset using xBD dataset. The model developed in this study can effectively detect damaged buildings and classify their damage levels by using high-resolution satellite imagery. The building damage detection results generated by the model provide better performance compared to the models in the existing literature. In addition, the domain adaptation results indicate that the model can be adapted to a new event with only little fine-tuning, which is critical for the application of the model for future events. In future work, we plan to improve the building boundaries using either GAN loss or exponential boundary loss, which could help to split different building instances.

The model and its outputs can inform emergency responders and decision makers of the locations of highly impacted buildings for source allocation of disaster response and recovery planning. For example, areas having more buildings identified as major damage may require more support in the aftermath of disasters. In addition to application to

building damage assessment, the proposed network architecture with hierarchical transformers can be used in other civil infrastructure and urban systems applications; for example, we expect this model architecture to perform well on problems such as road damage classification, structure change detection, and urban land cover change classification problems.

7 Acknowledgments

The authors would like to acknowledge funding support from the Texas A&M X-Grant Presidential Excellence Fund.

8 Code Availability

The code of the proposed model in this study is available at <https://github.com/nka77/DAHITra>

9 Data Availability

xBD dataset is publicly available at <https://xview2.org/dataset>. LEVIR-CD dataset can be acquired from <https://justchenhao.github.io/LEVIR/>. Ida-BD is publicly available on DesignSafe-CI at <https://www.designsafe-ci.org/data/browser/public/designsafe.storage.published/PRJ-3563>.

References

- Bandara, W. G. C., & Patel, V. M. (2022). *A transformer-based siamese network for change detection*. arXiv. Retrieved from <https://arxiv.org/abs/2201.01293>
- Beven II, J. L., Hagen, A., & Berg, R. (2022). *National Hurricane Center Tropical Cyclone Report - Hurricane Ida* (Tech. Rep. No. AL092021). National Hurricane Center. Retrieved from https://www.nhc.noaa.gov/data/tcr/AL092021_Ida.pdf
- Cao, Q. D., & Choe, Y. (2020). Building damage annotation on post-hurricane satellite imagery based on convolutional neural networks. *Natural Hazards*, 103(3), 3357–3376.
- Chen, H., Qi, Z., & Shi, Z. (2022). Remote sensing image change detection with transformers. *IEEE Transactions on Geoscience and Remote Sensing*, 60, 1-14.
- Cheng, C., Behzadan, A. H., & Noshadravan, A. (2021). Deep learning for post-hurricane aerial damage assessment of buildings. *Computer-Aided Civil and Infrastructure Engineering*, mice.12658. doi:10.1111/mice.12658
- Corbane, C., Carrion, D., Lemoine, G., & Broglia, M. (2011). Comparison of Damage Assessment Maps Derived from Very High Spatial Resolution Satellite and Aerial Imagery Produced for the Haiti 2010 Earthquake. *Earthquake Spectra*, 27(1_suppl1), 199–218.
- Fujita, A., Sakurada, K., Imaizumi, T., Ito, R., Hikosaka, S., & Nakamura, R. (2017). Damage detection from aerial images via convolutional neural networks. In *2017 Fifteenth IAPR International Conference on Machine Vision Applications (MVA)* (pp. 5–8).
- Gupta, R., Hosfelt, R., Sajeev, S., Patel, N., Goodman, B., Doshi, J., ... Gaston, M. E. (2019). xBD: A dataset for assessing building damage from satellite imagery. *CoRR*, abs/1911.09296. Retrieved from <http://arxiv.org/abs/1911.09296>
- Gupta, R., & Shah, M. (2021). Rescuenet: Joint building segmentation and damage assessment from satellite imagery. In *2020 25th international conference on pattern recognition (icpr)* (p. 4405-4411).
- Hao, H., Baireddy, S., Bartusiak, E. R., Konz, L., LaTourette, K., Gribbons, M., ... Comer, M. L. (2021). An attention-based system for damage assessment using satellite imagery. In *2021 IEEE International Geoscience and Remote Sensing Symposium IGARSS* (p. 4396-4399).
- Ku, J., Seo, J., & Jeon, T. (2020). *Dual-hrnet for building localization and damage classification*. Retrieved from https://github.com/SIAalytics/dual-hrnet/blob/master/figures/xView2_White_Paper_SI_Analytics.pdf
- Labelbox. (2022). *Labelbox*. Retrieved from <https://labelbox.com>
- Lee, C.-C., Kaur, N., Mahdavi-Amiri, A., & Mostafavi, A. (2022). *Ida-BD: pre- and post-disaster high-resolution satellite imagery for building damage assessment from Hurricane Ida*. Designsafe-CI. doi:10.17603/DS2-PD9H-6K05

- McCarthy, M. J., Jessen, B., Barry, M. J., Figueroa, M., McIntosh, J., Murray, T., . . . Muller-Karger, F. E. (2020). Mapping hurricane damage: A comparative analysis of satellite monitoring methods. *International Journal of Applied Earth Observation and Geoinformation*, *91*, 102134.
- Shen, Y., Zhu, S., Yang, T., Chen, C., Pan, D., Chen, J., . . . Du, Q. (2022). Bdanet: Multiscale convolutional neural network with cross-directional attention for building damage assessment from satellite images. *IEEE Transactions on Geoscience and Remote Sensing*, *60*, 1-14.
- Spencer, B. F., Hoskere, V., & Narazaki, Y. (2019). Advances in Computer Vision-Based Civil Infrastructure Inspection and Monitoring. *Engineering*, *5*(2), 199–222.
- Tong, X., Hong, Z., Liu, S., Zhang, X., Xie, H., Li, Z., . . . Bao, F. (2012). Building-damage detection using pre- and post-seismic high-resolution satellite stereo imagery: A case study of the May 2008 Wenchuan earthquake. *ISPRS Journal of Photogrammetry and Remote Sensing*, *68*, 13–27.
- Wang, M., & Deng, W. (2018). Deep visual domain adaptation: A survey. *Neurocomputing*, *312*, 135-153. doi:10.1016/j.neucom.2018.05.083
- Wang, N., Zhao, X., Zou, Z., Zhao, P., & Qi, F. (2020). Autonomous damage segmentation and measurement of glazed tiles in historic buildings via deep learning. *Computer-Aided Civil and Infrastructure Engineering*, *35*(3), 277–291. doi:10.1111/mice.12488
- Weber, E., & Kané, H. (2020). Building disaster damage assessment in satellite imagery with multi-temporal fusion. *CoRR*, *abs/2004.05525*. Retrieved from <https://arxiv.org/abs/2004.05525>
- Wu, B., Xu, C., Dai, X., Wan, A., Zhang, P., Yan, Z., . . . Vajda, P. (2021). Visual transformers: Where do transformers really belong in vision models? In *Proceedings of the IEEE/CVF International Conference on Computer Vision (ICCV)* (p. 599-609).
- Wu, C., Zhang, F., Xia, J., Xu, Y., & Li, G. (2021). Building damage detection using u-net with attention mechanism from pre- and post-disaster remote sensing datasets. *Remote Sensing*, *13*(5). doi:10.3390/rs13050905
- Zou, D., Zhang, M., Bai, Z., Liu, T., Zhou, A., Wang, X., . . . Zhang, S. (2022). Multicategory damage detection and safety assessment of post-earthquake reinforced concrete structures using deep learning. *Computer-Aided Civil and Infrastructure Engineering*, *37*(9), 1188–1204. doi:10.1111/mice.12815